Check for updates

Geophysical Research Letters

RESEARCH LETTER
10.1029/2020GL091719

Key Points:

- Both idealized and realistic numerical simulations uncover new properties of the transport tensor used to represent mesoscale tracer transports
- The full spatio-temporal complexity reveals strong time- and tracer-dependence, as well as the systematic presence of negative diffusivities
- The complexity of the eddy transports calls for reconsideration of how they are represented in models and estimated from observations

Supporting Information:

- Supporting Information S1

Correspondence to:
I. Kamenkovich,
ikamenkovich@miami.edu

Citation:
Kamenkovich, I., Berloff, P., Haigh, M., Sun, L., & Lu, Y. (2021). Complexity of mesoscale eddy diffusivity in the ocean. *Geophysical Research Letters*, *48*, e2020GL091719. https://doi.org/10.1029/2020GL091719

Received 18 SEP 2020
Accepted 22 DEC 2020

© 2020. American Geophysical Union. All Rights Reserved.

Complexity of Mesoscale Eddy Diffusivity in the Ocean

Igor Kamenkovich[1], Pavel Berloff[2,3], Michael Haigh[2], Luolin Sun[2], and Yueyang Lu[1]

[1]Rosenstiel School of Marine and Atmospheric Sciences, University of Miami, Miami, FL, USA, [2]Department of Mathematics, Imperial College London, London, UK, [3]Institute of Numerical Mathematics of the Russian Academy of Sciences, Moscow, Russia

Abstract Stirring of water by mesoscale currents ("eddies") leads to large-scale transport of many important oceanic properties ("tracers"). These eddy-induced transports can be related to the large-scale tracer gradients, using the concept of turbulent diffusion. The concept is widely used to describe these transports in the real ocean and to represent them in climate models. This study focuses on the inherent complexity of the corresponding coefficient tensor ("*K*-tensor") and its components, defined here in all its spatio-temporal complexity. Results demonstrate that this comprehensive *K*-tensor is space-, time-, direction- and tracer-dependent. Using numerical simulations with both idealized and comprehensive models of the Atlantic circulation, we show that these properties lead to upgradient eddy fluxes and the potential importance of all tensor components. The uncovered complexity of the eddy transports calls for reconsideration of how they are estimated in practice, included in the general circulation models and theoretically interpreted.

Plain Language Summary Mesoscale eddies, loosely defined as ocean currents on the spatial scales of tens to hundreds of kilometers, are ubiquitous in the World Ocean. Relentless stirring of water by these eddies leads to large-scale transport and redistribution of such important oceanic properties as heat, salinity, and anthropogenic carbon. The efficiency of this process has been conventionally described by turbulent ("eddy") diffusion. Our study focuses on the inherent complexity of the corresponding transport tensor, defined here in all its complexity, without any space and/or time averaging. Results from this study demonstrate that this transport tensor varies with location and time. Using numerical simulations with both simplified and realistic models of the North Atlantic circulation, we show that these properties lead to eddy fluxes that act to sharpen tracer fronts, rather than smooth them. We also show that all components of the comprehensive tensor are potentially important for tracer distributions, and, therefore, cannot be generally neglected. Our results further demonstrate that the comprehensive diffusivity tensor depends on the tracer that it is derived from. The uncovered complexity of the eddy transports calls for reconsideration of how they are estimated in practice, included in the general circulation models and theoretically interpreted.

1. Introduction

Mesoscale eddies, loosely defined as ocean currents on the spatial scales of tens to hundreds of kilometers, are ubiquitous in the World Ocean (Chelton et al., 2007). Relentless stirring of water by these eddies leads to large-scale transport and redistribution of many dynamically and climatically important oceanic properties ("tracers"), including heat, salinity, and anthropogenic carbon (McWilliams, 2008). As a result, mesoscale eddies play a key role in determining the current and future states of the World Ocean and the Earth Climate, as manifested by strong sensitivity of ocean and climate simulations to the magnitude and distribution of eddy transports (Gnanadesikan et al., 2013; McWilliams, 2008; Wiebe & Weaver, 1999). At the same time, vast majority of ocean components in modern climate models either completely miss the eddies or only partially resolve them (Adcroft et al., 2019; Delworth et al., 2012; Williams et al., 2015). The eddy-induced transports in these models need to be additionally expressed ("parameterized") in terms of known large-scale properties. This task requires a thorough study of eddy transport properties and their significance for tracer distributions. Below, we report on several new and important properties of the eddy transport using the framework of turbulent eddy diffusion, which is defined next.

By analogy between turbulent transport and molecular diffusion, the corresponding turbulent flux $F(x,y,z,t)$ of a tracer concentration c can be written as a linear function of the large-scale tracer gradient (Prandtl, 1925; Taylor, 1921; Vallis, 2017).

$$F = -K\nabla\langle c\rangle \tag{1}$$

where K will be referred to as "K-tensor" (also called "transport tensor" in literature) and the angle brackets denote the large-scale component of a field. This flux-gradient relation, with some common simplifications, has been traditionally used in numerical models to parameterize turbulent fluxes due to the important unresolved part of the flow. The divergence of the eddy flux enters the full tracer equation in these models, along with advection by the large-scale flow

$$\frac{\partial c}{\partial t} + \nabla\cdot\left(\langle u\rangle\langle c\rangle\right) = -\nabla\cdot F, \qquad \text{where } F = \langle u\rangle c' + u'\langle c\rangle + u'c' \tag{2}$$

Equation 2 can also be written for the large-scale tracer tendency $\partial\langle c\rangle/\partial t$, which introduces additional terms because $\langle\nabla uc\rangle \neq \nabla\langle uc\rangle$. In this study, we tried both formulations and arrived at the same conclusions. For simplicity, we assume that the tracer is conservative, thus ignoring sources and sinks and focus only on dynamically passive tracers, thus assuming that the ocean currents are not affected by c.

Because of the joint effect of planetary rotation and ocean stratification, the stirring of water by mesoscale eddies is primarily along neutral density surfaces (Iselin, 1939; Mcdougall, 1987; McDougall et al., 2014), which can be approximated by isopycnal (constant density) surfaces in the interior ocean. This is particularly convenient in this study, which uses isopycnal numerical models. Therefore, the focus here is on the lateral material transport. The general K-tensor in a two-dimensional (2D) flow can be written as a 2×2 matrix

$$K(x,y,t) = \begin{pmatrix} K_{xx} & K_{xy} \\ K_{yx} & K_{yy} \end{pmatrix}, \tag{3}$$

where the conventional Cartesian coordinates are used for convenience. Note that a pair of tracers is needed for a solution of Equation 1 and for that pair, the solution is exact and unique.

The seeming simplicity of the flux-gradient relation (Equation 1) hides the incredible complexity of the K-tensor. Only in purely homogeneous, stationary and isotropic turbulence are the off-diagonal tensor zero ($K_{xy} = K_{yx} = 0$) and the diagonal tensor elements are equal to each other ($K_{xx} = K_{yy}$). In realistic oceanic flows, all K-tensor elements are generally nonzero, distinct (i.e., the eddy-induced mixing is anisotropic) and vary in space and time (i.e., the mixing is inhomogeneous and nonstationary). Observation- and model-based estimates of the simplified eddy diffusivity exhibit strong dependence on depth, geographical location (Abernathey & Marshall, 2013; Cole et al., 2015; Canuto et al., 2019; Griesel et al., 2010; Groeskamp et al., 2020; Lumpkin et al., 2002; Marshall et al., 2006), and time (Busecke & Abernathey, 2019; Haigh et al., 2020). These estimates usually involve some spatio-temporal averaging and can be based on either drifter ("particle") trajectories or tracer distributions. Both particle-based statistics (Griesel et al., 2010; Kamenkovich et al., 2009, 2015; McClean et al., 2002; O'Dwyer et al., 2000; Rypina et al., 2012; Sallee et al., 2008) and tracer-based estimates (Abernathey et al., 2013; Bachman et al., 2017, 2020; Eden, 2007; Haigh et al., 2020) also exhibit significant anisotropy. This anisotropy is important in the typical oceanic case of strong eddies embedded in relatively weak large-scale circulation (Kamenkovich et al., 2015).

The diffusion approach (Equation 1) is built on an inherent assumption that the K-tensor is unique for any given turbulent flow. However, some model estimates report significant sensitivity of a simplified K-tensor to the tracer field (Abernathey et al., 2013; Bachman et al., 2020, 2015; Eden & Greatbatch, 2009; Haigh et al., 2020). This sensitivity complicates interpretation of the K-tensor because even the exact solution of Equation 1 for one particular pair of tracers will lead to biases in F for another set.

The other serious complication is that F contains some large nondivergent ("rotational") component (Haigh et al., 2020; Jayne & Marotzke, 2002; Marshall & Shutts, 1981) that does not affect tracer

distribution, because only divergence of the eddy fluxes matters, but influences K in the flux-gradient relation (Equation 1). The rotational flux can be tracer-dependent (Bachman et al., 2015) and can lead to negative diffusivities (Marshall & Shutts, 1981). The separation of F into rotational and divergent components via the Helmholtz decomposition is, unfortunately, not unique and depends on the boundary conditions (Fox-Kemper et al., 2003; Jayne & Marotzke, 2002; Maddison et al., 2015; Roberts & Marshall, 2000), which are usually known for the total F but not for its rotational and divergent components, separately. The need to remove the rotational component thus leads to another source of ambiguity in estimating the K-tensor.

This study describes the complexity of the eddy-induced transports, using the K-tensor framework in its entire spatio-temporal complexity, assuming neither temporal nor zonal averaging. The analysis explores tensor's dependence on tracer, importance of all its components, opposite signs of its diffusivities, and significant spatial inhomogeneity and temporal variability that cannot be removed by commonly applied spatio-temporal averaging. This complexity strongly suggests the need to expand the traditional flux-gradient relation of Equation 1 to include new functional and/or stochastic terms.

2. Numerical Simulations

Two types of simulations are used in this study to guarantee the robustness of conclusions. The first type is the idealized quasi geostrophic (QG) double-gyre flow. This flow contains all the essential elements of the mid-latitude North Atlantic or North Pacific: large-scale subpolar and subtropical gyres, separated by a coherent meandering jet, representing eastward extensions of the Gulf Stream and Kuroshio currents, and an ambient eddy field. The model is formulated in a square-box, flat-bottom ocean basin, which is a classical idealization that facilitates the analysis and numerical simulations (Haigh et al., 2020). The numerics employ the CABARET scheme (Karabasov et al., 2009) on a uniform Cartesian grid with 1025 by 1025 grid points and the grid spacing $\Delta x = \Delta y = 3.75$ km. The model has three isopycnal/isoneutral layers. The length of the tracer simulations is 180 days, and the circulation was preliminary span up until the statistical equilibrium.

The second model is a comprehensive, general circulation model (GCM) of the entire Atlantic, used in the "offline" regime, which means that tracers are simulated using previously computed daily physical fields, thus, making the model computationally very efficient (Kamenkovich et al., 2017). The physical variables used in offline models are calculated in a separate "online" simulation with the hybrid coordinate ocean model (HYCOM) (Bleck, 2002; Chassignet et al., 2003), which uses isopycnal coordinates in the open ocean and below the mixed layer. HYCOM's coordinate system dynamically transitions to other coordinate types (sigma- and z-coordinates) to provide optimal resolution in the surface-mixed layer, in high-latitude unstratified regions, and near coasts. The online simulation has a global domain with 1/12° spatial resolution; the horizontal grid is rectilinear south of 47°N followed by an Arctic bipolar patch. The vertical grid has 41 layers.

Both model solutions are initialized with 2D tracer configurations which initially are vertically uniform but have different horizontal profiles (see supporting information). The QG model is integrated for 180 days, while the GCM is used for several overlapping segments, 110 days each.

3. Tensor Calculation and Basic Properties

The definition of the large-scale circulation and large-scale tracer field is not unique, and the resulting K-tensor depends significantly on it. The mesoscale is not clearly separated from the large-scale in ocean models and observations (McWilliams, 2008), and an unambiguous definition of the eddies is missing. The large scales are often defined as long-term time mean (Vallis, 2017), although the utility of this definition is far from clear for transient tracers. Thus, a fundamental uncertainty in defining the eddies leads to uncertainty in defining the eddy diffusivity. This study defines mesoscale using spatial filtering, which is relevant to the task of spatial resolution of eddies in numerical models (Stanley et al., 2020). For example, the QG analysis in this study employs the low-pass spatial filtering <...> intended to remove scales shorter than 112.5 km (Rossby deformation radius is 40 km), while the GCM analysis uses a square filter width of

approximately 2° longitude. Large-scale GCM velocities are also averaged over 5 years for the most efficient separation of the large-scale circulation (Kamenkovich et al., 2017).

The flux-gradient relation can be solved exactly for any pair of independent tracers. In the QG simulations, we use 6 tracers that are initially linear (constant gradient) and 6 nonlinear tracers (15 independent pairs in each set). The linear tracers are of the form $ax + by + \gamma$, which means solving Equation 1 must produce a unique diffusivity tensor if the rotational component is properly removed. This is because any linear tracer can be expressed as a linear combination of only 2 independent tracers. In the GCM simulations, we use four independent tracers (six tracer pairs).

The rotational component is removed from each tracer flux, using the Helmholtz decomposition (Lau & Wallace, 1979):

$$\nabla \cdot F = \nabla^2 \Phi, \nabla \times F = \nabla^2 \Psi$$

$$F = F_{\text{div}} + F_{\text{rot}}$$

$$F_{\text{div}} = \nabla \Phi, F_{\text{rot}} = \nabla \times \Psi \tag{4}$$

In the above equations, Φ is the potential that corresponds to the divergent flux component F_{div} whereas Ψ is the streamfunction that corresponds to the rotational component F_{rot}. In the QG simulations, we adopt the approach of Maddison et al. (2015) and set $\Phi = 0$ at the lateral boundaries, which minimizes the magnitude of F_{div}. GCM simulations have open boundaries in the north and south, and a different approach is used. We chose to use the optimization technique with Tikhonov regularization (Li et al., 2006), which minimizes the opposing nonrotational and nondivergent components in F_{div} and $\left(F - F_{\text{div}}\right)$. Note that $\nabla \cdot F_{\text{div}} = \nabla \cdot F$ regardless of the boundary conditions used in the Helmholtz decomposition, although the K-tensor is derived from F_{div} and, thus, is highly sensitive to the choice of the boundary conditions.

The K-tensor can be decomposed into the symmetric and antisymmetric components with distinct physical interpretations (Griffies, 1998; Plumb & Mahlman, 1987):

$$K = K_s + K_a = \begin{pmatrix} K_{xx} & S_{12} \\ S_{12} & K_{yy} \end{pmatrix} + \begin{pmatrix} 0 & A_{12} \\ -A_{12} & 0 \end{pmatrix}, \qquad S_{12} = \frac{1}{2}\left(K_{xy} + K_{yx}\right),$$
$$A_{12} = \frac{1}{2}\left(K_{xy} - K_{yx}\right). \tag{5}$$

The symmetric K_{s} and antisymmetric K_{a} parts are traditionally referred to as the "diffusion tensor" and "advection tensor," respectively. The diffusion tensor can be conveniently diagonalized by rotating the local coordinate through an angle θ (Rypina et al., 2012; Kamenkovich et al., 2015).

$$K_{\text{s}} = \begin{pmatrix} \lambda_1 & 0 \\ 0 & \lambda_2 \end{pmatrix} \tag{6}$$

The angle θ defines the direction of the maximal tracer diffusivity, and the first eigenvalue λ_1 is the eddy diffusivity in this direction. The second eigenvalue λ_2 corresponds to the diffusivity in the direction perpendicular to the maximal one. Both eigenvalues are real and will be referred to as diffusivities in this study. The advection tensor corresponds to advection of tracers by nondivergent eddy-induced velocities.

When the eddy-induced stirring (K-tensor) is isotropic and homogeneous, these two components of the full tensor correspond to the divergent (zero curl and nonzero divergence) and rotational (zero divergence and nonzero curl) components, $-K_{\text{s}}\nabla\langle c\rangle$ and $-K_{\text{a}}\nabla\langle c\rangle$, respectively. Since the rotational component does not affect tracer distributions, only K_s needs to be calculated in this case. In a more general case like ours,

both K_s and K_a are important, and the antisymmetric part has nonzero divergence for the inhomogeneous tensor: $\nabla \cdot K_a \nabla\langle c\rangle = J\left(A,\langle c\rangle\right) \neq 0$. Moreover, it is possible to show that the curl of the symmetric part is also nonzero, $\nabla \times K_s \nabla\langle c\rangle \neq 0$, if K_s is anisotropic ($K_{xx} \neq K_{yy}$) or inhomogeneous. For example, our QG estimates show that the r.m.s. of the divergence of $K_s\nabla\langle c\rangle$ and $K_a\nabla\langle c\rangle$ are both 2.5×10^{-9} s^{-1} (tracer is unitless), and the curl of these components is 6.5×10^{3} s^{-1} and 6.7×10^{3} s^{-1}, respectively. Because the rotational component is exactly zero in the full F_{div}, the rotational components in the symmetric and antisymmetric parts cancel each other.

3.1. Polarity and Time Dependence

An intriguing new feature of the comprehensive K_s is the persistence of pairs of positive and negative diffusivities (eigenvalues) λ_1 and λ_2 (Figures 1 and 2), which we will refer to as "polarity." Many previous studies excluded negative diffusivities, either by using asymptotic estimates based on particle trajectories (Berloff et al., 2002; Kamenkovich et al., 2015; Rypina et al., 2012) or by explicitly constraining diffusivities to be non-negative (Bachman et al., 2020). Polar diffusivities imply that the tracer concentration anomalies are being stretched in one direction (direction of positive diffusivity, defined by the angle θ) and squeezed in the direction normal to that (direction of negative diffusivity), leading to transient filamentation of the tracer field. Moreover, the polarity, which is ubiquitous in both QG and GCM solutions, is a robust feature of the instantaneous flow and is observed regardless of whether and how the rotational component of F is removed.

All components of the comprehensive tensor have significant time dependence, with the standard deviations comparable with and exceeding the corresponding time-mean values (Figure 3). The uncovered time dependence has important implications not only for transient tracer behavior, but also for time-mean tracer structure. The latter point can be illustrated by the time-average eddy flux $\overline{F_{\text{div}}}$. To see this, we can write the time average of Equation 1 in two different ways:

$$\overline{F_{\text{div}}} = -\overline{K}\nabla\overline{\langle c\rangle} - \overline{K'\nabla\langle c'\rangle}, K' = K - \overline{K}, c' = c - \overline{c}$$

or

$$\overline{F_{\text{div}}} = -\tilde{K}\nabla\overline{\langle c\rangle}, \tag{7}$$

where $\tilde{K}$ is the K-tensor defined from the time-mean eddy fluxes and tracer gradients. The above relation implies that (i) K' can be at least as important as $\overline{K}$, as suggested in Figure 3; and (ii) $\tilde{K}$ is different from $\overline{K}$. Both properties are confirmed by our calculations. The most practical approach for the parametrization is then unclear. Obtaining accurate estimates of time-dependent $K'\left(x,y,t\right)$ is problematic in practice, whereas using $\tilde{K}$ can distort the important variability in F_{div} and the simulated tracer field.

Due to the nonstationary nature of K_s, its eigenvalues (diffusivities) and the corresponding angle θ both change in time. Although the polarity is reduced in $\overline{K_s}$ and $\widetilde{K_s}$, it continues to be observed even in these fields (not shown), which implies that eddies lead to persistent filamentation. As the sharpening of tracer gradients cannot continue forever, the effects of eddies have to be eventually balanced by the large-scale advection and small-scale diffusion, and persistent upgradient tracer fluxes are indeed possible under certain conditions (Wilson & Williams, 2006). Persistent upgradient eddy potential vorticity fluxes, which correspond to negative diffusivity in the cross-stream direction have been reported in the eastward extensions of the Kuroshio (Waterman et al., 2011; Waterman & Jayne, 2011) and Gulf Stream (Shevchenko & Berloff, 2015); these studies, however, did not report the K-tensor and the sign of the along-flow diffusivity. Another possibility is that negative eigenvalues are associated with nondivergent, rotational component of $K_s\nabla c$. Regardless of the origin and interpretation of the polarity, neglecting the negative values will lead to biases in the instantaneous eddy fluxes and tracer distributions. Although these biases can be partially averaged out over time, the implications for tracer variability need to be carefully assessed.

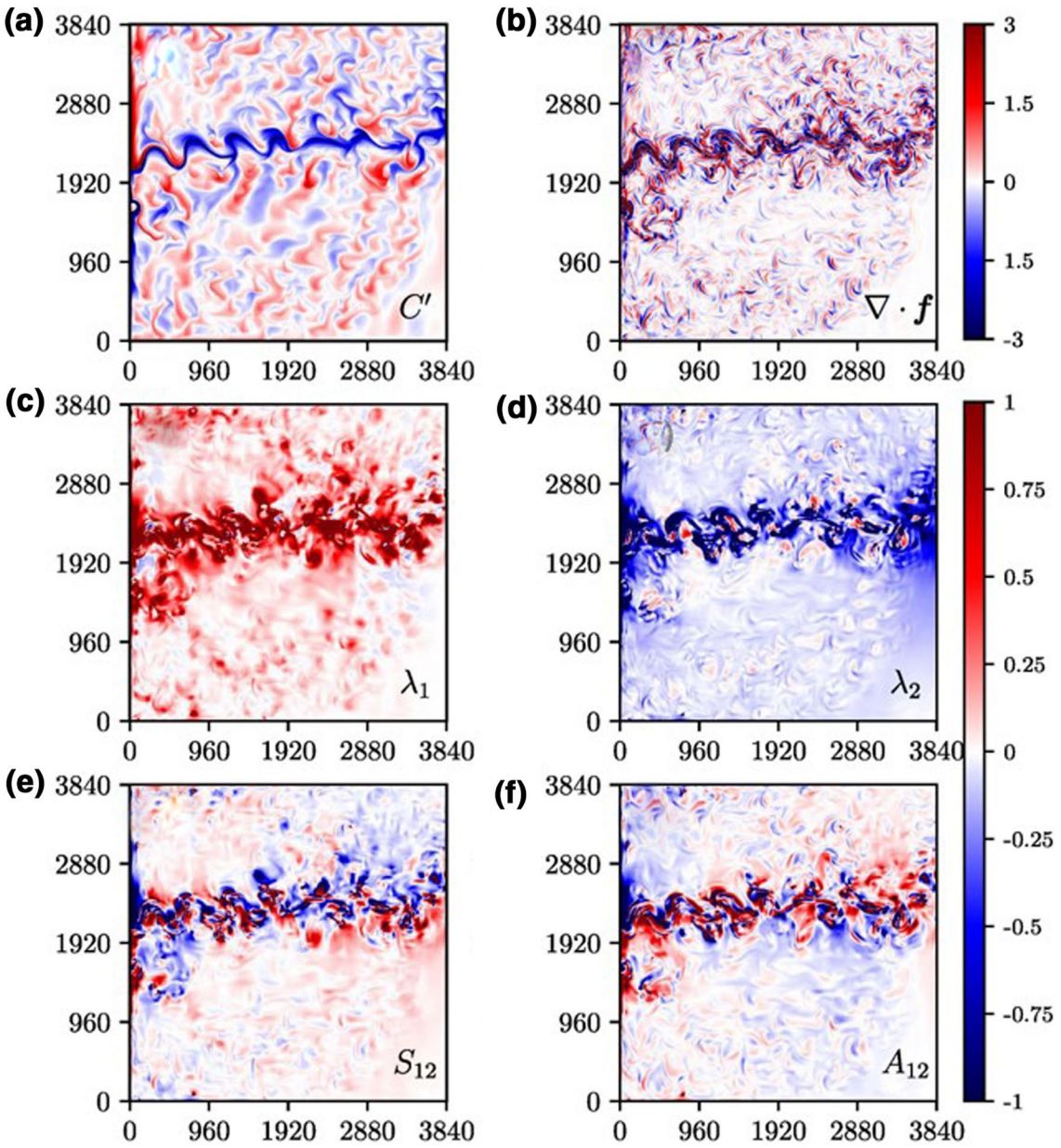

Figure 1. Results of the QG simulations at day 183: (a) tracer anomaly $c' = c(x,y,t) - c(x,y,0)$; (b) divergence of the tracer flux (tracer units times 10^{-16} s^{-1}); (c)-(d) eigenvalues of K_s and (e)-(f) off-diagonal terms of the K_s and K_a (units are 10^4 m^2 s^{-1}). Axis units are km.

3.2. Dependence on Tracers

Another unexpected property of the diffusion tensor K_s is its dependence on the tracer field, which implies that $K_s(x,y,t)$ is not uniquely determined by the flow and exists for each tracer pair separately. To illustrate this property in our study, we consider the entire ensemble of the diffusivities λ_1, calculated among all possible pairs of tracers. The resultant ensemble standard deviation $S^{(\lambda)}$ exceeds the ensemble mean in most of the domain for both the QG and GCM simulations (Figures 4 and 5). Even more significantly, the spread in the values of the diffusive-flux divergence $\nabla \cdot K_s \nabla \langle c \rangle$ is large (not shown).

The rotational component can be naturally suspected of being the cause of the above nonuniqueness of the K-tensor. Nevertheless, our results demonstrate that the nonuniqueness (as measured by $S^{[\lambda]}$) is not

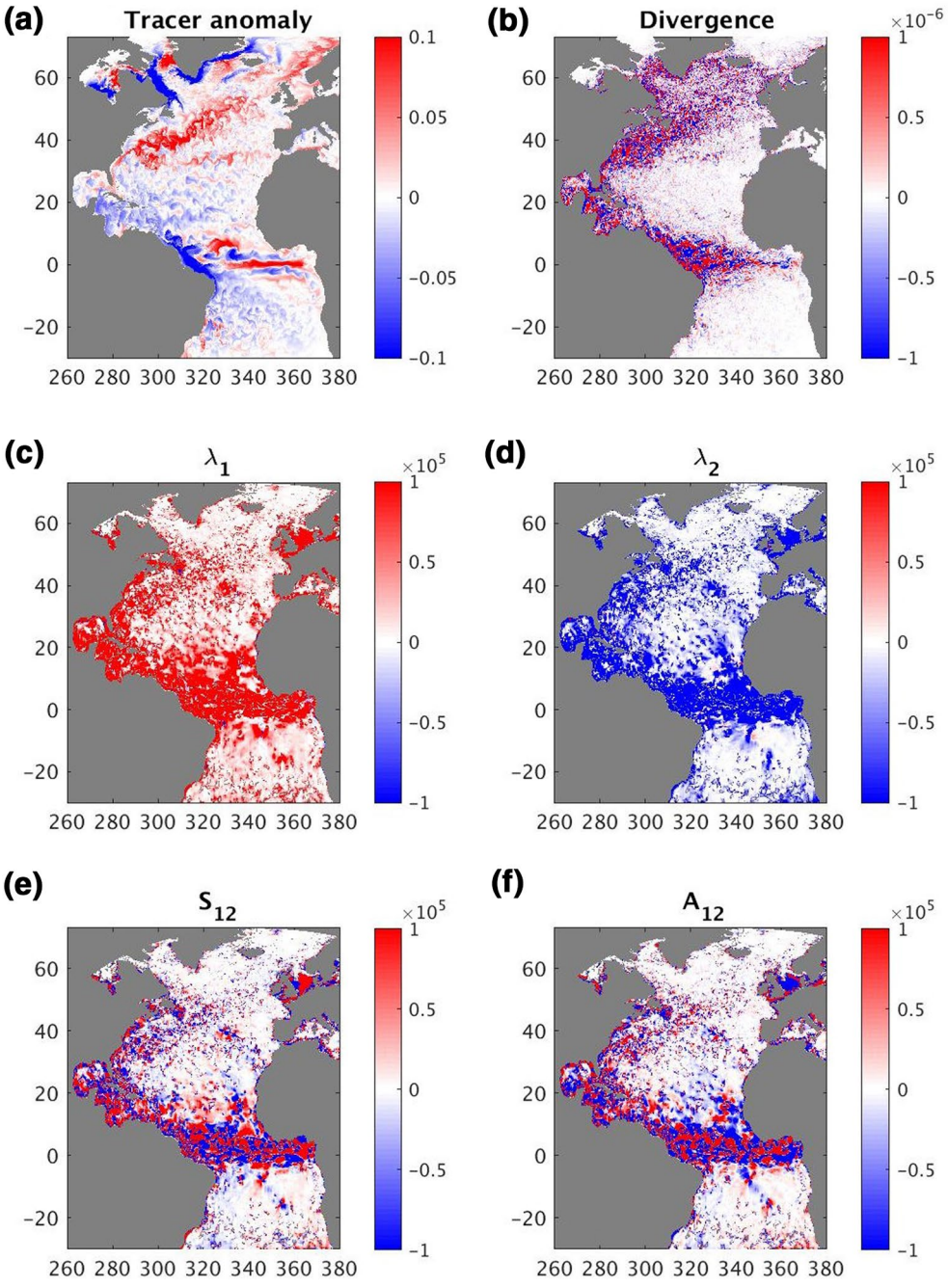

Figure 2. Results of the GCM simulations, layer 17 (depth of approximately 110-140 m): (a) tracer anomaly $c' = c(x,y,t) - c(x,y,0)$ at day 350, year 1 (tracer is unitless); (b) divergence of the tracer flux (units are s^{-1}) averaged over days 341–350 of year 1, smoothed for presentation purposes; (c)-(d) eigenvalues of K_s and (e)-(f) off-diagonal terms of K_s and K_a (units are $m^2\ s^{-1}$), derived from the eddy fluxes and tracer gradients averaged over days 341–350 of year 1. Note large values in the tropics due to weak tracer gradients and, possibly, long Rossby deformation radius. Regions near the open boundaries, where the tracer concentrations are initially set to zero are masked. Axes are degrees longitude/latitude.

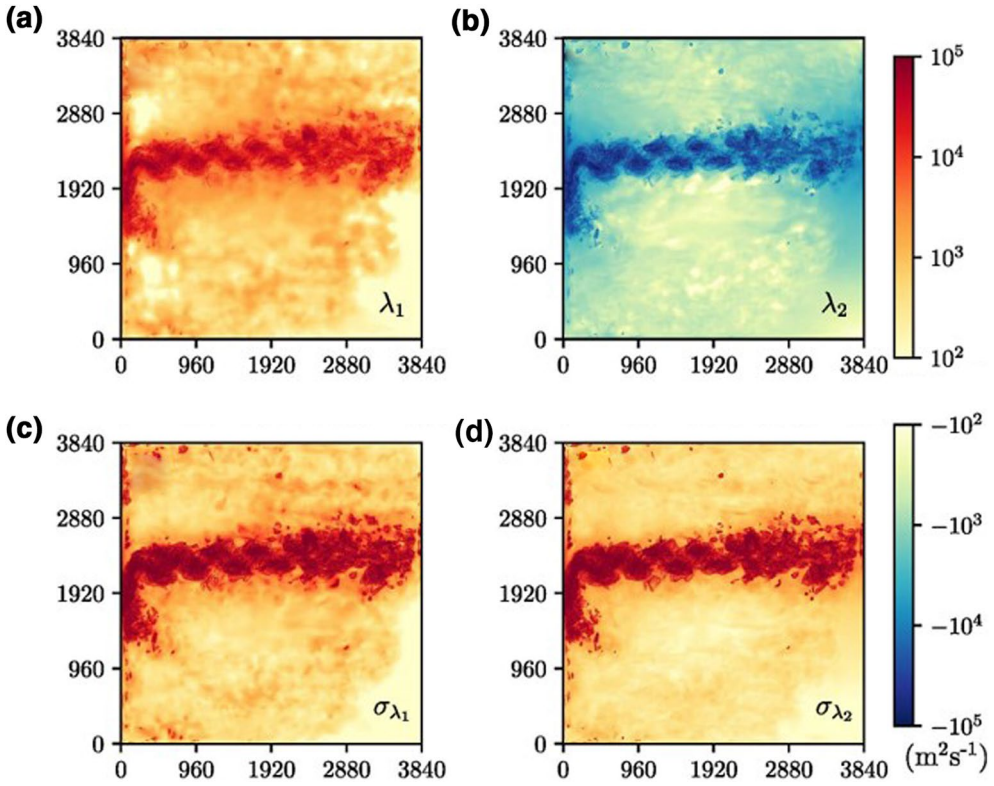

Figure 3. Temporal variability in the eigenvalues (diffusivities) λ_1 and λ_2 of the diffusion tensor K_s in the QG simulations over the period of 183 days. Panels (a-b) show the time-mean values, panels (c-d) show the standard deviations. Time-means of eigenvalues are over 183 days. Axes are km.

significantly increased when the rotational component is added for a general set of tracers: $S^{(\lambda)}$is similar in magnitude for F and F_{div} in both the QG and GCM simulations (Figures 4c and 4d and Figures 5a and 5b). To confirm that we can indeed remove the rotational component, we repeat the above analysis for the initially linear (constant gradient) tracers in the QG simulations, which must lead to the same diffusivity from F_{div} for all tracer pairs (see supporting information). Indeed, in this case $S^{(\lambda)}$ for F_{div} is orders of magnitude smaller than the same quantity for F. (Figures 4a and 4b). We conclude that the presence of the rotational component cannot be the main cause of nonuniqueness.

4. Implications for Eddy Parameterization and Diffusivity Estimates

Using the exact solution for $K(x,y,t)$ from (Equation 1) would lead to an accurate representation of the eddy-flux divergence for the given tracer pair, and regardless of how and whether the rotational component is removed. However, this is not how the problem of parameterization is formulated. An ultimate goal of the diffusion-based description of the eddy-induced transports is parameterization of $K(x,y,t)$ in terms of large-scale currents and stratification, that is, arrival at some generalized "turbulence closure." The corresponding approximate tensor $K_p \approx K(x,y,t)$ is intended to reproduce the most important effects of eddies on the large-scale tracer fields, without explicitly resolving the mesoscale. The uncovered complexity of the K-tensor implies that the parameterized eddy flux divergence $-\nabla \cdot K_p \nabla\langle c\rangle$ will inevitably contain biases with respect to $\nabla \cdot F$, but the significance of these biases for tracer distribution remains to be studied. These biases can be particularly hard to control, since the diffusive flux will have a large rotational component which affects the K-tensor estimates, according to our analysis. Since an exact match between K_p and K is practically impossible, it is important to estimate what properties of the K-tensor are most important for tracer distribution. This study describes several examples of such properties.

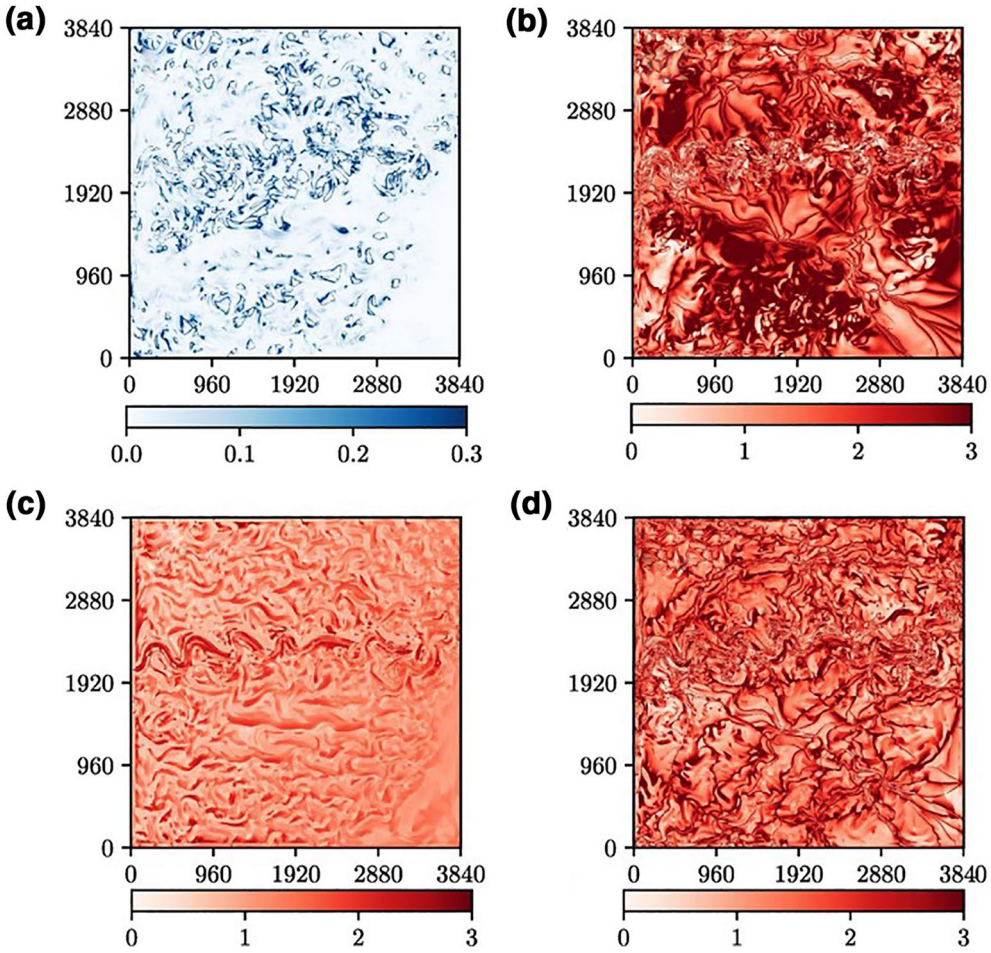

Figure 4. Nonuniqueness of the K-tensor (tracer dependence) in the QG simulations (day 183), for the ensemble of 15 tracer pairs. It is shown as the ensemble standard deviation $S^{(\lambda)}$ divided by the ensemble mean for the first eigenvalue λ_1, calculated for F_{div} (left column) and **F** (right column): (a-b) Linear tracers in the QG model; (c-d) Nonlinear tracers in the QG model. Axes are km.

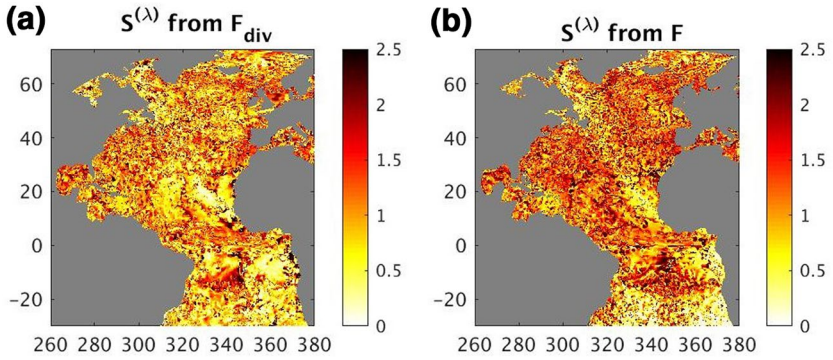

Figure 5. Nonuniqueness (tracer dependence) of the K-tensor in the HYbrid Coordinate Ocean Model (HYCOM) simulations, for the ensemble of six tracer pairs. It is shown as the ensemble standard deviation $S^{(\lambda)}$ divided by the ensemble mean for the first eigenvalue λ_1, calculated for F_{div} (left column) and F (right column). The tensor is derived from the eddy fluxes and tracer gradients averaged over days 341–350 of year 1, layer 17. Axes are degrees in longitude/latitude.

The K-tensor depends on the flow decomposition (definition of the large-scale <...>), which is loosely defined in most cases. This study defines mesoscale based on spatial scales, which is more directly relevant to the issue of its parameterization in numerical models. The spatial filter characteristics cannot, however, be easily derived from model resolution alone, since it is unclear to what extent different dynamical scales are actually resolved. The K-tensor is also nonstationary, and a meaningful definition of K_p will depend on the time scales of large-scale tracer variability, potentially emerging from the state dependence in K_p (Adcroft et al., 2019; Stanley et al., 2020). The analysis of the dominant spatial and temporal scales will need to be carried out in each particular case. Negative diffusivities (eigenvalues of the diffusion tensor) and the potential importance of all tensor components dramatically complicate the definition of the closure. These negative diffusivities are, however, transient, and the corresponding direction of spreading constantly changes in time. The importance of this variability needs to be assessed. In addition, the effects of negative eigenvalues can potentially be fully compensated by the flux resulting from the advection tensor, which is divergent and, thus, also plays a role in tracer distribution. Although the K-tensor polarity reflects the actual properties of eddy fluxes, negative diffusivity in numerical simulation should be implemented with caution, in order to avoid singularities. Observation-based estimates, on the other hand, present additional challenges. Given the discovered complexity, obtaining accurate estimates of K from drifter and float trajectories (Lagrangian observations) appears highly problematic, because these asymptotic and spatially nonlocal methods will not be able to accurately capture the spatial and temporal variability of the K-tensor, as well as its negative eigenvalues and its advective component.

Finally, the comprehensive K-tensor is a function of the tracer field, formally violating assumptions of the classical, tracer-independent flux-gradient relation. A practical approach to this problem is to use multitracer ensemble-averaged estimates of K_s (Abernathey et al., 2013; Bachman et al., 2017, 2020), but the corresponding and unavoidable biases for each given tracer pair remain to be assessed and understood. Although the nonuniqueness may be potentially alleviated by using long-term time averages, the errors in instantaneous parameterized eddy fluxes can lead to large biases in simulations of such important transient tracers as heat anomalies and anthropogenic carbon.

Negative diffusivities and tracer dependence clearly illustrate the fact that the stirring driven by mesoscale currents is dramatically more complex than the molecular diffusion, which is used to motivate the flux-gradient representation. An alternative solution is to expand the traditional flux-gradient representation of the eddy flux by adding new, nondiffusive and/or nongradient terms. Such expansion can involve terms that explicitly depend on either the tracer concentration or its curvature, as well as purely stochastic components. Another alternative is to represent K-tensor as a stochastic process, as it has been done in the past for other transport parameters (Berloff & McWilliams, 2003; Grooms, 2016). Finally, approximating eddy flux divergence, instead of eddy fluxes themselves, will help to avoid ambiguity associated with the presence of the rotational component.

Since the most important properties and aspects of K_p remain to be identified, we do not yet know to what extent they are affected by the full tensor properties described in this study. Although it is tempting to conclude that only the direct resolution of the mesoscale can lead to accurate tracer simulations, we must realize that the task of its parameterization will remain relevant for some time. The presented complexity and nonuniqueness of the K-tensor suggest that the flux-gradient relationship is not suitable for representing eddy-induced fluxes in terms of large-scale properties and alternative types of parameterizations may be needed.

Acknowledgments
I. Kamenkovich and Y. Lu were supported by NOAA grant NA16OAR4310165 and NSF grant 1849990. The authors declare no conflicts or competing interests. P. Berloff gratefully acknowledges funding by NERC, UK Grants *NE/R*011567/1 and *NE/T*002220/1, and by Leverhulme Trust, UK Grant *RPG*−2019−024, and by the Moscow Center for Fundamental and Applied Mathematics (supported by the Agreement 075-15−2019−1624 with the Ministry of Education and Science of the Russian Federation). I. Kamenkovich would like to thank Zulema Garraffo for the continuous help with the offline HYCOM model; P. Berloff, M. Haigh, and L. Sun would like to thank James McWilliams for fruitful discussions on the topics of this study.

Data Availability Statement

Model data used to produce figures in this study are available from https://doi.org/10.17604/a1q6-d035.

References

Abernathey, R., Ferreira, D., & Klocker, A. (2013). Diagnostics of isopycnal mixing in a circumpolar channel. *Ocean Modelling*, *72*, 1–16. https://doi.org/10.1016/j.ocemod.2013.07.004

Abernathey, R., & Marshall, J. (2013). Global surface eddy diffusivities derived from satellite altimetry. *Journal of Geophysical Research*, *118*(2), 901–916. https://doi.org/10.1002/jgrc.20066

Adcroft, A., Anderson, W., Balaji, V., Blanton, C., Bushuk, M., Dufour, C. O., et al. (2019). The GFDL Global Ocean and Sea Ice Model OM4.0: Model description and simulation features. *Journal of Advances in Modeling Earth Systems*, *11*(10), 3167–3211. https://doi.org/10.1029/2019ms001726

Bachman, S. D., Fox-Kemper, B., & Bryan, F. O. (2015). A tracer-based inversion method for diagnosing eddy-induced diffusivity and advection. *Ocean Modelling*, *86*, 1–14. https://doi.org/10.1016/j.ocemod.2014.11.006

Bachman, S. D., Fox-Kemper, B., & Bryan, F. O. (2020). A Diagnosis of anisotropic eddy diffusion from a high-resolution global ocean model. *Journal of Advances in Modeling Earth Systems*, *12*(2). https://doi.org/10.1029/2019MS001904

Bachman, S. D., Marshall, D. P., Maddison, J. R., & Mak, J. (2017). Evaluation of a scalar eddy transport coefficient based on geometric constraints. *Ocean Modelling*, *109*, 44–54. https://doi.org/10.1016/j.ocemod.2016.12.004

Berloff, P. S., & McWilliams, J. C. (2003). Material transport in oceanic gyres. Part III: Randomized stochastic models. *Journal of Physical Oceanography*, *33*(7), 1416–1445. https://doi.org/10.1175/1520-0485(2003)033<1416:Mtiogp>2.0.Co;2

Berloff, P. S., McWilliams, J., & Bracco, A. (2002), Material transport in oceanic gyres. Part I: Phenomenology, *Journal of Physical Oceanography*, *32*, 764–796, https://doi.org/10.1175/1520-0485(2002)032<0764:MTIOGP>2.0.CO;2

Bleck, R. (2002). An Oceanic general circulation model framed in hybrid isopycnic-Cartesian coordinates. *Ocean Modelling*, *4*(2), 219. https://doi.org/10.1016/S1463-5003(01)00017-8

Busecke, J. J. M., & Abernathey, R. P. (2019). Ocean mesoscale mixing linked to climate variability. *Science Advances*, *5*(1). https://doi.org/10.1126/sciadv.aav5014

Canuto, V. M., Cheng, Y., Howard, A. M., & Dubovikov, M. S. (2019). Three-dimensional, space-dependent mesoscale diffusivity: Derivation and implications. *Journal of Physical Oceanography*, *49*(4), 1055–1074. https://doi.org/10.1175/Jpo-D-18-0123.1

Chassignet, E. P., Smith, L. T., Halliwell, G. R., & Bleck, R. (2003). North Atlantic simulations with the hybrid coordinate ocean model (HYCOM): Impact of the vertical coordinate choice, reference pressure, and thermobaricity. *Journal of Physical Oceanography*, *33*(12), 2504–2526. https://doi.org/10.1175/1520-0485(2003)033<2504:Naswth>2.0.Co;2

Chelton, D. B., Schlax, M. G., Samelson, R. M., & de Szoeke, R. A. (2007), Global observations of large oceanic eddies, *Geophysical Research Letters*, *34*(15), L15606. https://doi.org/10.1029/2007gl030812

Cole, S. T., Wortham, C., Kunze, E., & Owens, W. B. (2015). Eddy stirring and horizontal diffusivity from Argo float observations: Geographic and depth variability. *Geophysical Research Letters*, *42*(10), 3989–3997. https://doi.org/10.1002/2015gl063827

Delworth, T. L., Rosati, A., Anderson, W., Adcroft, A. J., Balaji, V., Benson, R., et al. (2012). Simulated climate and climate change in the GFDL CM2.5 high-resolution coupled climate model. *Journal of Climate*, *25*(8), 2755–2781. https://doi.org/10.1175/Jcli-D-11-00316.1

Eden, C. (2007). Eddy length scales in the North Atlantic Ocean. *Journal of Geophysical Research*, *112*(C6), C06004. https://doi.org/10.1029/2006jc003901

Eden, C., & Greatbatch, R. J. (2009). A diagnosis of isopycnal mixing by mesoscale eddies. *Ocean Modelling*, *27*(1–2), 98–106. https://doi.org/10.1016/j.ocemod.2008.12.002

Fox-Kemper, B., Ferrari, R., & Pedlosky, J. (2003). On the indeterminacy of rotational and divergent eddy fluxes. *Journal of Physical Oceanography*, *33*(2), 478–483. https://doi.org/10.1175/1520-0485(2003)033<0478:Otiora>2.0.Co;2

Gnanadesikan, A., Bianchi, D., & Pradal, M. A. (2013). Critical role for mesoscale eddy diffusion in supplying oxygen to hypoxic ocean waters. *Geophysical Research Letters*, *40*(19), 5194–5198. https://doi.org/10.1002/grl.50998

Griesel, A., Gille, S. T., Sprintall, J., McClean, J. L., LaCasce, J. H., & Maltrud, M. E. (2010). Isopycnal diffusivities in the Antarctic Circumpolar Current inferred from Lagrangian floats in an eddying model. *Journal of Geophysical Research*, *115*(C6), C06006. https://doi.org/10.1029/2009jc005821

Griffies, S. M. (1998), The Gent-McWilliams skew flux, *Journal of Physical Oceanography*, *28*(5), 831–841. https://doi.org/10.1175/1520-0485(1998)028<0831:Tgmsf>2.0.Co;2

Groeskamp, S., LaCasce, J. H., McDougall, T. J., & Rogé, M. (2020). Full-depth global estimates of ocean mesoscale eddy mixing from observations and theory. *Geophysical Research Letters*, *47*(18), e2020GL089425. https://doi.org/10.1029/2020GL089425

Grooms, I. (2016). A Gaussian-product stochastic Gent-McWilliams parameterization. *Ocean Modelling*, *106*, 27–43. https://doi.org/10.1016/j.ocemod.2016.09.005

Haigh, M., Sun, L., Shevchenko, I., & Berloff, P. (2020). Tracer-based estimates of eddy-induced diffusivities. *Deep-Sea Research Part I*, *160*, 1–8. https://doi.org/10.1016/j.dsr.2020.103264

Iselin, C. O. D. (1939). The influence of vertical and lateral turbulence on the characteristics of the waters at mid depths. *Eos Transactions American Geophysical Union*, *20*(3), 414–417. https://doi.org/10.1029/TR020i003p00414

Jayne, S. R., & Marotzke, J. (2002). The oceanic eddy heat transport. *Journal of Physical Oceanography*, *32*(12), 3328–3345. https://doi.org/10.1175/1520-0485(2002)032<3328:Toeht>2.0.Co;2

Kamenkovich, I., Berloff, P., & Pedlosky, J. (2009). Anisotropic material transport by eddies and eddy-driven currents in a model of the North Atlantic. *Journal of Physical Oceanography*, *39*(12), 3162–3175. https://doi.org/10.1175/2009jpo4239.1

Kamenkovich, I., Garraffo, Z., Pennel, R., & Fine, R. A. (2017). Importance of mesoscale eddies and mean circulation in ventilation of the Southern Ocean. *Journal of Geophysical Research: Oceans*, *122*(4), 2724–2741. https://doi.org/10.1002/2016jc012292

Kamenkovich, I., Rypina, I. I., & Berloff, P. (2015). Properties and origins of the anisotropic eddy-induced transport in the North Atlantic. *Journal of Physical Oceanography*, *45*(3), 778–791. https://doi.org/10.1175/Jpo-D-14-0164.1

Karabasov, S. A., Berloff, P. S., & Goloviznin, V. M. (2009). CABARET in the ocean gyres. *Ocean Modelling*, *30*(2–3), 155–168. https://doi.org/10.1016/j.ocemod.2009.06.009

Lau, N. C., & Wallace, J. M. (1979), Distribution of horizontal transports by transient eddies in the Northern Hemisphere wintertime circulation, *Journal of the Atmospheric Sciences*, *36*(10), 1844–1861. https://doi.org/10.1175/1520-0469(1979)036<1844:Otdoht>2.0.Co;2

Li, Z. J., Chao, Y., & McWilliams, J. C. (2006), Computation of the streamfunction and velocity potential for limited and irregular domains, *Monthly Weather Review*, *134*(11), 3384–3394. https://doi.org/10.1175/Mwr3249.1

Lumpkin, R., Treguier, A. M., & Speer, K. (2002), Lagrangian eddy scales in the Northern Atlantic Ocean, *Journal of Physical Oceanography*, *32*(9), 2425–2440. https://doi.org/10.1175/1520-0485-32.9.2425

Maddison, J. R., Marshall, D. P., & Shipton, J. (2015). On the dynamical influence of ocean eddy potential vorticity fluxes. *Ocean Modelling*, *92*, 169–182. https://doi.org/10.1016/j.ocemod.2015.06.003

Marshall, J., Shuckburgh, E., Jones, H., & Hill, C. (2006), Estimates and implications of surface eddy diffusivity in the Southern Ocean derived from tracer transport, *Journal of Physical Oceanography*, *36*(9), 1806–1821. https://doi.org/10.1175/Jpo2949.1

Marshall, J., & Shutts, G. (1981), A note on rotational and divergent eddy fluxes, *Journal of Physical Oceanography*, *11*(12), 1677–1680. https://doi.org/10.1175/1520-0485(1981)011<1677:Anorad>2.0.Co;2

McClean, J. L., Poulain, P. M., Pelton, J. W., & Maltrud, M. E. (2002), Eulerian and lagrangian statistics from surface drifters and a high-resolution POP simulation in the North Atlantic, *Journal of Physical Oceanography*, *32*(9), 2472–2491. https://doi.org/10.1175/1520-0485-32.9.2472

Mcdougall, T. J. (1987), Neutral surfaces, *Journal of Physical Oceanography*, *17*(11), 1950–1964. https://doi.org/10.1175/1520-0485(1987)017<1950:Ns>2.0.Co;2

McDougall, T. J., Groeskamp, S., & Griffies, S. M. (2014). On geometrical aspects of interior ocean mixing. *Journal of Physical Oceanography*, *44*(8), 2164–2175. https://doi.org/10.1175/Jpo-D-13-0270.1

McWilliams, J. (2008). The nature and consequences of oceanic eddies. In M. Hecht, & H. Hasumi (Eds.), *Eddy-resolving ocean modeling* (pp. 131–147). AGU Monographs.

O'Dwyer, J., Williams, R. G., LaCasce, J. H., & Speer, K. G. (2000). Does the potential vorticity distribution constrain the spreading of floats in the North Atlantic? *Journal of Physical Oceanography*, *30*(4), 721–732. https://doi.org/10.1175/1520-0485(2000)030<0721:Dtpvdc>2.0.Co;2

Plumb, R. A., & Mahlman, J. D. (1987). The zonally averaged transport characteristics of the GFDL general-circulation transport model. *Journal of the Atmospheric Sciences*, *44*(2), 298–327. https://doi.org/10.1175/1520-0469(1987)044<0298:Tzatco>2.0.Co;2

Prandtl (1925). Bericht über untersuchungen zur ausgebildeten turbulenz. *Zeitschrift für Angewandte Mathematik und Mechanik*, *5*, 136–139. https://doi.org/10.1002/zamm.19250050212

Roberts, M. J., & Marshall, D. P. (2000). On the validity of down-gradient eddy closures in ocean models. *Journal of Geophysical Research*, *105*(C12), 28613–28627. https://doi.org/10.1029/1999jc000041

Rypina, I. I., Kamenkovich, I., Berloff, P., & Pratt, L. J. (2012). Eddy-induced particle dispersion in the near-surface North Atlantic. *Journal of Physical Oceanography*, *42*(12), 2206–2228. https://doi.org/10.1175/Jpo-D-11-0191.1

Sallee, J. B., Speer, K., Morrow, R., & Lumpkin, R. (2008). An estimate of Lagrangian eddy statistics and diffusion in the mixed layer of the Southern Ocean. *Journal of Marine Research*, *66*(4), 441–463. https://doi.org/10.1357/002224008787157458

Shevchenko, I. V., & Berloff, P. S. (2015). Multi-layer quasi-geostrophic ocean dynamics in Eddy-resolving regimes. *Ocean Modelling*, *94*, 1–14. https://doi.org/10.1016/j.ocemod.2015.07.018

Stanley, Z., Bachman, S. D., & Grooms, I. (2020). Vertical structure of ocean mesoscale eddies with implications for parameterizations of tracer transport. *Journal of Advances in Modeling Earth Systems*, *12*(10), e2020MS002151. https://doi.org/10.1029/2020MS002151

Taylor (1921). Diffusion by continuous movements. *Proceedings of the London Mathematical Society*, *20*, 196–211.

Vallis, G. (2017). *Atmospheric and oceanic fluid dynamics* (1st ed.). Cambridge University Press. https://doi.org/10.2277/0521849691

Waterman, S., Hogg, N. G., & Jayne, S. R. (2011). Eddy-mean flow interaction in the Kuroshio extension region. *Journal of Physical Oceanography*, *41*(6), 1182–1208. https://doi.org/10.1175/2010jpo4564.1

Waterman, S., & Jayne, S. R. (2011). Eddy-mean flow interactions in the along-stream development of a western boundary current jet: An idealized model study. *Journal of Physical Oceanography*, *41*(4), 682–707. https://doi.org/10.1175/2010jpo4477.1

Wiebe, E. C., & Weaver, A. J. (1999), On the sensitivity of global warming experiments to the parametrisation of sub-grid scale ocean mixing, *Climate Dynamics*, *15*(12), 875–893. https://doi.org/10.1007/s003820050319

Williams, K. D., Harris, C. M., Bodas-Salcedo, A., Camp, J., Comer, R. E., Copsey, D., et al. (2015). The met office global coupled model 2.0 (GC2) configuration. *Geoscientific Model Development*, *8*(5), 1509–1524. https://doi.org/10.5194/gmd-8-1509-2015

Wilson, C., & Williams, R. G. (2006), When are eddy tracer fluxes directed downgradient? *Journal of Physical Oceanography*, *36*(2), 189–201. https://doi.org/10.1175/Jpo2841.1